Molecular Therapy
Nucleic Acids
Original Article

# Fluorinated Nucleotide Modifications Modulate Allele Selectivity of SNP-Targeting Antisense Oligonucleotides

Michael E. Østergaard,[1] Josh Nichols,[1] Timothy A. Dwight,[2] Walt Lima,[1] Michael E. Jung,[2] Eric E. Swayze,[1] and Punit P. Seth[1]

[1]Ionis Pharmaceuticals, 2855 Gazelle Court, Carlsbad, CA 92010, USA; [2]Department of Chemistry and Biochemistry, University of California Los Angeles, Los Angeles, CA 90095, USA

**Antisense oligonucleotides (ASOs) have the potential to discriminate between subtle RNA mismatches such as SNPs. Certain mismatches, however, allow ASOs to bind at physiological conditions and result in RNA cleavage mediated by RNase H. We showed that replacing DNA nucleotides in the gap region of an ASO with other chemical modification can improve allele selectivity. Herein, we systematically substitute every position in the gap region of an ASO targeting *huntingtin* gene (HTT) with fluorinated nucleotides. Potency is determined in cell culture against mutant HTT (mtHTT) and wild-type HTT (wtHTT) mRNA and RNase H cleavage intensities, and patterns are investigated. This study profiled five different fluorinated nucleotides and showed them to have predictable, site-specific effects on RNase H cleavage, and the cleavage patterns were rationalized from a published X-ray structure of human RNase H1. The results herein can be used as a guide for future projects where ASO discrimination of SNPs is important.**

## INTRODUCTION

Antisense oligonucleotides (ASOs) bind to their cognate mRNA by Watson-Crick base-pairing and modulate its processing to produce a pharmacological effect.[1] ASOs that function through the RNase H-based antisense mechanism were first discovered more than three decades ago when administration of exogenous short DNA oligonucleotides was shown to direct RNA reduction in cells.[2] Since those initial reports, extensive studies have been performed to improve the drug-like properties of RNase H active ASOs.[3] This body of work resulted in use of phosphorothioate-modified oligonucleotides[4] and development of the "gapmer" design, i.e., a DNA gap region of 8–16 nt flanked on either end with 2′-modified nucleotides.[4] More than 35 ASOs with this general design are currently in various stages of clinical trials and one ASO, Kynamro, was recently approved for the treatment of homozygous familial hypercholesterolemia.[5]

Following introduction of the gapmer design,[6,7] the majority of studies aimed at improving ASO properties have focused on modifying the wing chemistry. 2′-Modified nucleotides, such as 2′-*O*-methoxyethyl RNA (MOE), which enhance ASO RNA-binding affinity and metabolic stability, have been extensively employed.[8] Replacing some or all of the MOE nucleotides in the wings with modifications such as locked nucleic acid (LNA) or *S*-constrained ethyl (cEt), which further enhance RNA-binding affinity, provided ASO designs with improved activity in animal models.[9,10]

In contrast to modification of the wing region, introducing chemical modifications in the gap region of RNase H active ASOs has been investigated less extensively.[11,12] We recently showed that introducing chemical modifications like 2-thio-deoxythymidine[13] and 5′-substituted DNA analogs[14] in the gap region of ASOs can enhance the discrimination of SNPs between two alleles in the *huntingtin* gene. The resulting ASOs showed potent reduction of mutant HTT (mtHTT) mRNA and protein in patient fibroblasts and in a mouse model of Huntington's disease (HD),[15] an autosomal dominant disorder that is thought to result from expansion of a polyglutamine-encoding CAG tract in the *huntingtin* gene. Allele-selective reduction of mtHTT by directly targeting the CAG repeat has also been reported.[16]

As part of the above effort, we also showed that introducing chemical modifications such as 2′-fluoro RNA (FRNA) or 2′-arabino fluoro RNA (FANA) near the 5′ end of the gap region in ASO control (CNTR) (Figure 1) can modulate allele selectivity.[17] FRNA and FANA differ only in the relative configuration of the fluorine atom at the 2′-position of the nucleotide furanose ring. However, the highly electronegative fluorine atom produces local changes in the conformation of the nucleotide furanose ring,[18] which can affect the biological properties of the modified ASOs.[19]

To further understand how fluorinated modifications in the gap region can modulate the allele selectivity of SNP-targeting ASOs, we sequentially replaced each DNA nucleotide in ASO CNTR with FRNA or FANA. FRNA is an RNA-analog adopting a C3′-*endo* conformation, whereas FANA adopts an unusual O4′-*endo*

Received 7 October 2016; accepted 2 February 2017;
http://dx.doi.org/10.1016/j.omtn.2017.02.001.

**Correspondence:** Michael E. Østergaard, Ionis Pharmaceuticals, 2855 Gazelle Court, Carlsbad, CA 92010, USA.
**E-mail:** moesterg@ionisph.com

 

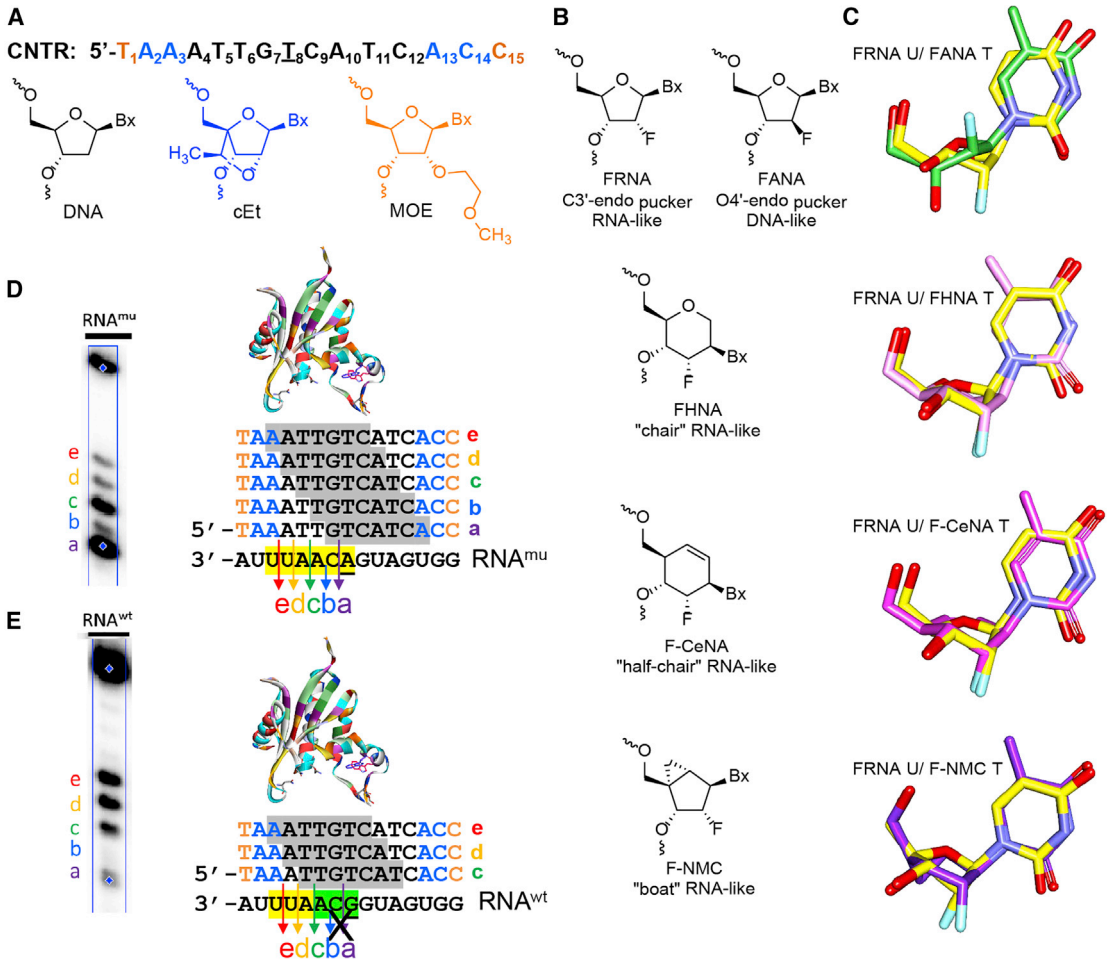


**Figure 1. ASO Design and 7-nt Footprint of the Catalytic Domain of RNase H1 to the DNA Strand of a DNA-RNA Heteroduplex**

(A) Sequence and structure of control ASO (CNTR). (B and C) Chemical structure and preferred sugar conformation of fluorinated nucleosides examined. (D and E) The unique, but overlapping, 7-nt footprint on ASO CNTR for cleavage sites a, b, c, d, and e on (D) mtHTT RNA and (E) wtHTT RNA, respectively. The central T:G mismatch (underlined) ablates cleavage sites a and b on wtHTT RNA.

conformation (Figures 1B and 1C)[20] and is one of the very few nucleotide modifications reported to increase RNA cleavage by RNase H1.[21,22] In addition, we also investigated the effect of replacing DNA nucleotides with other fluorinated modifications such as 2′-fluoro-hexitol nucleic acid (FHNA), 2′-fluoro cyclohexenyl nucleic acid (F-CeNA), and 2′-fluoro *N*-methanocarba nucleic acid (F-NMC) for modulating allele selectivity. FHNA and F-CeNA are ring-expanded analogs of FRNA. However, the six-membered hexitol ring in FHNA is more rigid and mimics the RNA-like C3′-*endo* conformation of the furanose ring (Figures 1B and 1C).[23] In contrast, the cyclohexenyl ring in F-CeNA is more flexible and was shown to assume either the DNA- or RNA-like sugar conformation depending on the sequence context on its incorporation.[24] The 3.1.0 ring system in F-NMC is locked in the RNA-like C3′-*endo* conformation.[25] In this report, we show that introducing fluorinated modifications within the gap region can modulate the cleavage of the ASO-RNA heteroduplexes by human RNase H1, and that this can produce profound changes in allele selectivity when targeting SNPs with gapmer ASOs.

## RESULTS AND DISCUSSION

### ASO Design

We selected a 3-9-3 gapmer ASO with mixed MOE/cEt wings as a starting point because it exhibits good potency and intermediate allele selectivity (ASO CNTR, 9-fold selectivity; Figure 1A).[26] Each fluorinated nucleotide was then walked systematically through the gap to examine effect on potency and selectivity in cell culture and to investigate RNase H cleavage patterns and determine relative amounts of RNA cleavage (for F-CeNA and F-NMC, we only had access to the pyrimidine analogs).

We had previously characterized the cleavage patterns produced by recombinant human RNase H1 for ASO duplexes with mtHTT

**A**

| Sequence | FRNA muHTT $IC_{50}$ (μM) | FRNA wtHTT $IC_{50}$ (μM) | FRNA Selectivity | FHNA muHTT $IC_{50}$ (μM) | FHNA wtHTT $IC_{50}$ (μM) | FHNA Selectivity | FANA muHTT $IC_{50}$ (μM) | FANA wtHTT $IC_{50}$ (μM) | FANA Selectivity |
|---|---|---|---|---|---|---|---|---|---|
| TAAATTGTCATCACC | 0.31 | 2.8 | 9 | 0.31 | 2.8 | 9 | 0.31 | 2.8 | 9 |
| TAAATTGTCATCACC | 0.28 | 4.2 | 15 | 0.20 | >10 | >50 | 0.21 | 4.0 | 19 |
| TAAATTGTCATCACC | 0.15 | 4.4 | 29 | 0.24 | >10 | >42 | 0.05 | 0.35 | 5 |
| TAAATTGTCATCACC | 0.77 | >10 | >13 | 0.75 | >10 | >13 | 0.11 | 1.21 | 11 |
| TAAATTGTCATCACC | 0.94 | >10 | >11 | 1.7 | >10 | >6 | 0.07 | 1.89 | 25 |
| TAAATTGTCATCACC | 0.24 | 0.96 | 4 | 0.24 | 4.8 | 20 | 0.20 | 7.0 | 35 |
| TAAATTGTCATCACC | 0.16 | 0.80 | 5 | 0.22 | 4.2 | 19 | 0.09 | 1.6 | 16 |
| TAAATTGTCATCACC | 0.20 | >10 | >50 | 0.30 | 6.3 | 21 | 0.20 | >10 | >50 |
| TAAATTGTCATCACC | 0.35 | 6.3 | 18 | 0.38 | 4.2 | 11 | 0.22 | 6.2 | 26 |
| TAAATTGTCATCACC | 0.07 | 1.3 | 18 | 0.09 | 0.45 | 5 | 0.10 | 3.2 | 30 |

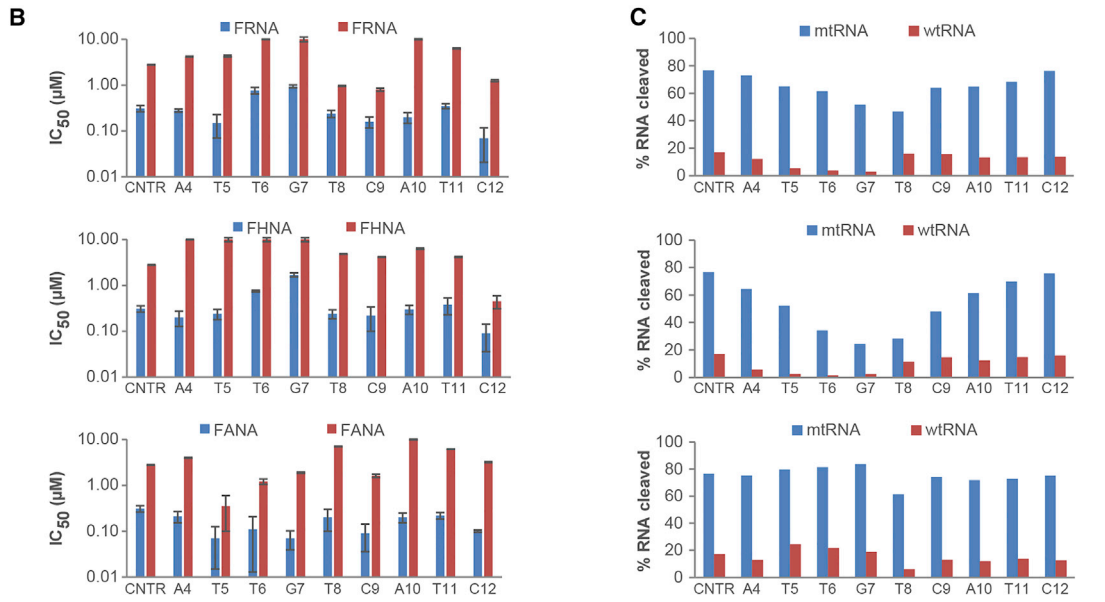


**Figure 2. Overview of ASO Cell Culture Potencies and Human RNase H1 Activity for ASO:RNA Duplexes**

(A) Summary of sequence, $IC_{50}$, and selectivity data for reducing mtHTT and wtHTT mRNA in human HD fibroblast (GM04022) using FRNA, FHNA, or FANA gap-modified ASOs. (B and C) Plot of $IC_{50}$ values in cells (B) versus total cleavage of mtHTT (blue bars) and wtHTT (red bars) RNA after incubation of ASO:RNA heteroduplexes with human RNase H1 (C).

RNA and wild-type HTT (wtHTT) RNA, representing the mtHTT and wtHTT mRNA, respectively (Figures 1D and 1E).[17] Five cleavage sites (a, b, c, d, and e) were identified on mtHTT RNA, whereas only three cleavage sites were detected on wtHTT RNA. ASO CNTR has a T:G mismatch with wtHTT RNA corresponding to the SNP site in the HTT mRNA, which ablates cleavage sites a and b on wtHTT RNA. The loss of RNase H1 cleavage sites reduces degradation of the wtHTT mRNA and provides a rationale for the modest selectivity observed with this ASO in patient-derived fibroblast cells and in mice bearing the human HTT transgene.[26]

Previous work by Nowotny et al.[27] had shown that the catalytic domain of human RNase H1 has a unique 7-nt footprint (Figures 1D and 1E, gray shaded region on ASO) on the DNA-RNA heteroduplex for a given cleavage site on the RNA strand. It was anticipated that introducing modifications at every position in the gap region could have a unique and differential impact on the individual cleavage sites because the modification would be located at a different position in the footprint for each cleavage site.

### Potency toward Complementary mtHTT and G Mismatched wtHTT RNA in Cell Culture

ASOs were tested in GM04022 fibroblast cells heterozygous at SNP rs7685686 (A-to-G mismatch). ASOs were transfected using electroporation, and RNA knockdown was evaluated 24 hr posttreatment using an allele-selective quantitative real time polymerase chain reaction (rtPCR) approach that allows simultaneous monitoring of mtHTT and wtHTT RNA reductions.[17] Chemical modification and position in the gap have pronounced effect on potency against mtHTT (Figure 2). Moving FRNA 1 or 2 nt into the gap results in slightly improved potency relative to control ASO (Figure 2B, position A4 and T5); however, further walking 1 and 2 nt into the gap

led to significant reductions in potency (position T6 and G7). Interestingly, positioning of an FRNA modification in the middle of the gap (position T8) restores the potency relative to control ASO. Further moving of FRNA through the gap had only minor effects on potency except at the last position (C12), where potency is improved. Potency against T:G mismatched wtHTT is also very position dependent, but trends are not similar to on-target potencies. FRNA allele selectivity is improved (i.e., wtHTT potency is reduced) upon moving the modification from the 5′-gap junction toward the center (Figure 2, top, position 4–7); however, positioning FRNA across from the mismatch (T8) reduces selectivity as compared with the control ASO. Further moving FRNA to the 3′ part of the gap leads to high selectivity at position A10 and low selectivity at positions C9 and C12.

Moving FHNA through the gap has similar but more pronounced effects relative to FRNA (Figure 2). Potencies against mtHTT are in most cases reduced as compared with FRNA at the same position and only at a few positions similar to FRNA (at positions A4, T8, and C12). Inhibitor concentration where target is reduced by 50% ($IC_{50}$) for wtHTT are generally higher for FHNA relative to FRNA, which in most cases results in better allele selectivity. It is important to note that general trends when moving FRNA and FHNA through the gap are similar against mtHTT, as well as wtHTT (Figures 2B and 2C). The similar properties but more pronounced effects when comparing FHNA with FRNA can be rationalized by comparing their conformations (Figure 1C). Although FHNA features a six-membered sugar ring, it positions the nucleobase, *O*3′-, and *O*5′-substituents very similar to a 3′-*endo* furanose nucleotide, and because of the rigid cyclohexane chair conformation FHNA behaves similar to 2′,4′-constrained nucleotides like LNA.[23]

FANA exhibits properties that are markedly different relative to the RNA-like modifications. Potency against complementary mtHTT RNA is similar or better than the control ASO at every position in the gap (Figure 2A). This is in line with previous reports showing that FANA is one of a handful of chemically modified nucleotides that increase potency of ASOs when positioned in the gap.[28] Generally, potency against mismatched wtHTT is also increased relative to control, but there are two notable exceptions: FANA at position A10 is exhibiting excellent selectivity; interestingly, FRNA and FHNA are also very selective at this position. Also, positioning FANA across from the SNP (at T8) results in improved allele selectivity, which is especially interesting because a large number of modifications were previously evaluated at this position, but FANA is the only one that significantly improves allele selectivity.[17] It is also worth noting that although FANA generally improves potency for both mtHTT and wtHTT, in most cases the allele selectivity is reduced or similar to the control ASO (Figure 2A).

### Human RNase H1 RNA Cleavage and Comparison with In Vitro Data

The very position-dependent effects on cell culture RNA reduction likely arise from differential interactions with RNase H1. Therefore, to better understand the cell culture data, we measured human RNase H1-mediated RNA cleavage for ASOs duplexed with either 19-mer complementary RNA (mtHTT) or G mismatched RNA (wtHTT).

There is a very general trend when walking FRNA and FHNA through the gap with complementary RNA: as the modification is walked toward the center, less total RNA is cleaved, with the least amount cleaved when modifying position T8 (Figure 2C). This observation is consistent with previous reports that most chemically modified nucleotides are disruptive toward RNase H-mediated cleavage.[11,12] At most positions, however, the reduction in total RNA cleavage is small, and it is possible that small changes will have little, if any, effect in biological systems where ASOs can behave in a catalytic manner to degrade RNA.[29,30] FANA again behaves differently and exhibits similar or increased RNA cleavage at all positions except when positioned at T8.

RNase H1-mediated RNA cleavage has very distinct trends for each modified nucleotide against mtHTT RNA, whereas it is more complicated against RNA with a centrally positioned G mismatch (wtRNA). FRNA and FHNA have similar trends, but the magnitude is different and FHNA has the most pronounced effects. When moving the modification from the 5′ end of the gap toward the center, reduced wtHTT RNA is cleaved (from A4 to G7; Figure 2D); however, modifying position T8 results in wtHTT RNA cleavage similar to control ASO. Further walking the modification toward the 3′ end of the gap has minor effects on RNA cleavage. FANA substitution results in similar or increased wtHTT RNA cleavage, which is especially notable at positions T5, T6, and G7. The only position where FANA substitution results in considerably less wtHTT RNA cleavage is across from the SNP (position T8); unfortunately, this position also has reduced mtHTT RNA cleavage, although cell culture potency is similar to control ASO.

Good correlation between cell culture potency and human RNase H1 cleavage will make it much easier to develop more mismatch-selective ASO designs because biochemical RNase H-mediated RNA cleavage assays are much simpler, faster, and give better signal-to-noise ratios relative to cell culture and animal experiments. For FHNA there is good linear correlation for wtHTT reduction, whereas mtHTT reduction shows little correlation. In general, there is good correlation between cell culture potency and human RNase H1 cleavage when comparing only the 5′ end of the gap (A4, T5, T6, and G7), but little overall linear correlation when modifying the 3′ end of the gap. The 5′ end of the gap is where the catalytic domain of human RNase H1 binds the heteroduplex.[27] It is possible that other factors in the cell are important for human RNase H1 interactions with the 3′ end of the gap.[31] Notably, the RNase H biochemical assay does not explain the good selectivity of any of the modifications when substituted at position A10 (Figure 2A) or the good selectivity exhibited by FANA when inserted across from the SNP site. ASO potency, however, is affected by many factors in addition to RNase H. ASO binding to intracellular proteins has been shown in some cases to alter potency[32] and, in particular, oligonucleotides incorporating fluorinated nucleotides occasionally exhibit enhanced binding to certain

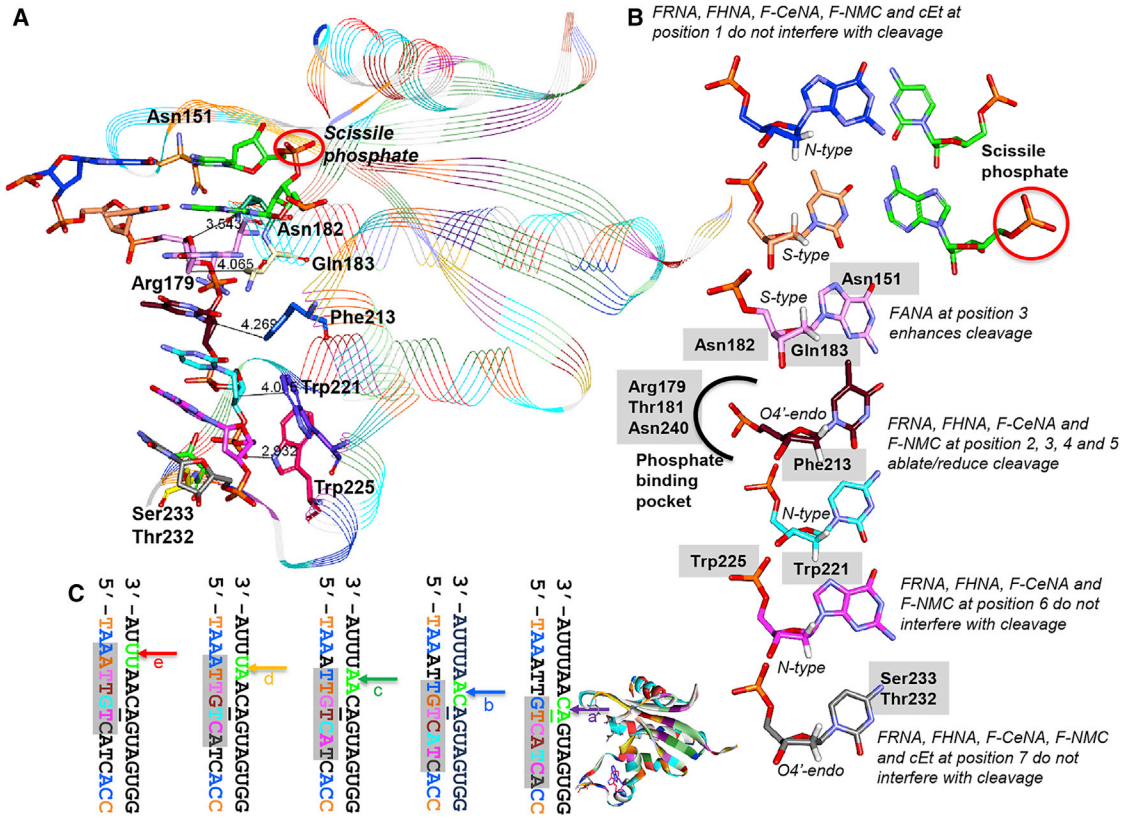


**Figure 3. Important Interactions between the Catalytic Domain of RNase H1 and the DNA Strand of a DNA-RNA Heteroduplex**

(A) The 7-nt footprint of the RNase H1 catalytic domain on the DNA strand for a given cleavage site (scissile phosphate). For the RNA strand (green carbons), only the 2 nt flanking the cleavage site are shown for clarity. (B) Conformational analysis and positional preference of the sugar puckers of the individual nucleotides in the 7-nt footprint. (C) The unique, but overlapping, 7-nt footprint on ASO CNTR for cleavage sites a, b, c, d, and e on mtHTT RNA. Every nucleotide is located at a different position in the footprint for the individual cleavage sites. For example, G7 is located at positions 1, 2, 3, 4, and 5 of the footprint for cleavage sites a, b, c, d, and e, respectively.

proteins.[33] Furthermore, it cannot be ruled out that chemical modification patterns can affect ASO uptake pathways.[34]

### Structural Analysis of the RNase H1 Cleavage Footprint for Gap-Modified ASOs

Human RNase H1 is a ubiquitously expressed enzyme that is comprised of three domains: catalytic, RNA-binding, and linker domains. The crystal structures of the catalytic and RNA-binding domains of human RNase H1 bound to DNA-RNA heteroduplexes have been described by Nowotny et al.[27] and were used to better understand the cleavage patterns observed in our experiments. The catalytic domain of human RNase H1 has a unique 7-nt footprint on the DNA-RNA heteroduplex for every individual cleavage site (Figures 3A and 3B). As a result, each nucleotide in the DNA strand will be located at a different position within the footprint based on the register in which the enzyme binds the heteroduplex (Figure 3C).

The catalytic domain of human RNase H1 makes several key contacts with the DNA and RNA strands of the heteroduplex (Figures 3A and 3B). The side chains of amino acids Asn151, Asn182, and Gln183 make several key H-bonding interactions with the nucleobases in the major groove. As a result, introducing nucleobase modifications such as 2-thio dT can disrupt specific cleavage sites depending on their position of incorporation in the ASO gap region.[13] The enzyme also makes key interactions with a phosphodiester linkage of the DNA strand within the phosphate binding pocket formed by amino acids Arg179, Thr181, and Asn240. Another key site of interaction is within the hydrophobic DNA-binding channel formed by the aromatic amino acids Phe213, Trp221, and Trp225. The aromatic side chains of these amino acids make close hydrophobic contacts with the bottom face of the DNA sugars. This provides specificity for DNA over RNA as the 2′-hydroxyl groups in RNA disrupt the hydrophobic contacts. Lastly, the enzyme makes a weak contact (Ser233) with the non-Watson-Crick face of the nucleobase at the last position of the footprint. This contact can be disrupted using bulky C5-modified pyrimidine nucleobases.[13]

The enzyme also produces numerous structural distortions in the DNA strand, which provide insights into why certain modifications

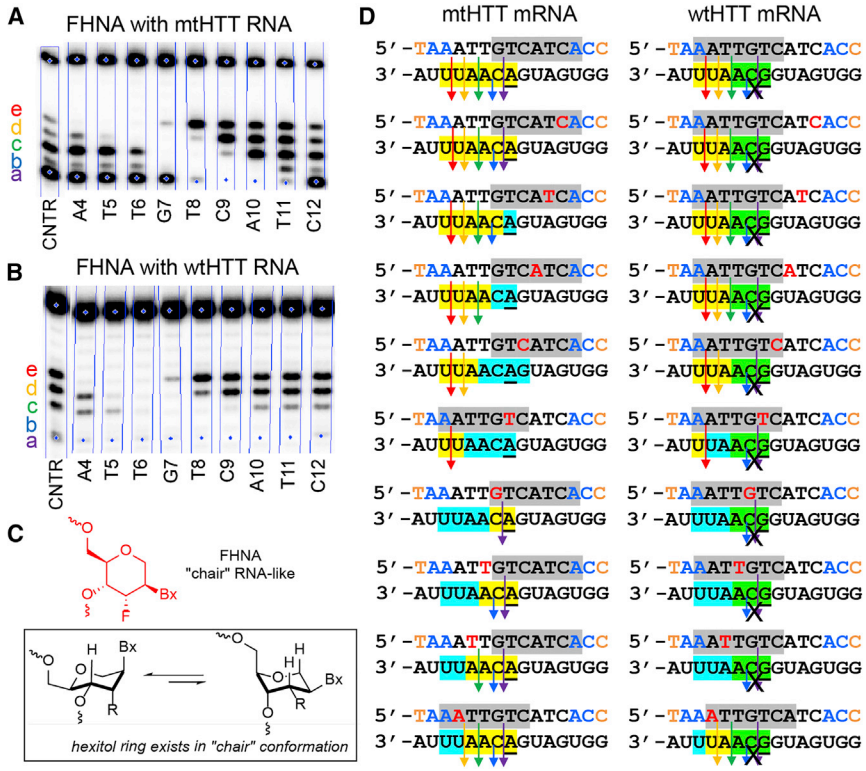


**Figure 4. RNase H Cleavage Patterns for FHNA Gap-Modified ASOs**

(A and B) Analysis of human RNase H1 cleavage patterns for FHNA gap-modified ASOs on (A) mtHTT RNA and (B) wtHTT RNA. (C) Structure and conformational equilibrium of the six-membered hexitol ring of FHNA. (D) Detailed analysis of the 7-nt footprint (gray shaded) on (D) ASO/mtHTT RNA and ASO/wtHTT RNA. The red letters depict position of FHNA nucleotide, and the cleavage sites on the RNA are shown using arrows. The yellow shaded areas indicate sites where RNase H1 is able to cleave the RNA strand, and the blue shaded areas indicate sites where FHNA ablates cleavage by RNase H1. The green shaded areas indicate sites where cleavage is ablated by the T:G mismatch corresponding to the SNP site.

are tolerated at specific positions in the gap region, but not at others (Figure 3B). For example, the DNA sugar of the first nucleotide of the footprint for a given cleavage site is in an RNA-like C3′-*endo* conformation. The DNA sugars of the second and third nucleotides are in the canonical DNA-like C2′-*endo* sugar pucker, whereas the DNA sugar of the fourth nucleotide is in a conformation that resembles O4′-*endo*. The conformation of the DNA sugars of nt 5 and 6 resemble an RNA-like C3′-*endo* sugar pucker, whereas the DNA sugar of nt 7 appears to be somewhat flexible. The paradoxical requirement for the DNA sugars at positions 4, 5, and 6 to be in an RNA-like conformation is better understood from a structural perspective. The RNA-like conformation positions the 3′-phosphodiester linkages in a pseudo-equatorial orientation that facilitates closer hydrophobic contacts with the bottom face of the DNA sugars. Lastly, the complex structural requirements are further complicated as each nucleotide in the gap region is located at a different position within the 7-nt footprint for any given cleavage site (Figure 3C).

### Analysis of Cleavage Patterns for FHNA Gap-Modified ASOs in Matched and Mismatched Duplexes

Introduction of FHNA at the 3′ edge of the gap region (C12) has no noticeable impact on the cleavage pattern relative to the control ASO CNTR with a 9-base DNA gap (Figures 4A and 4B). FHNA at C12 corresponds to position 6 for cleavage site "a" and position 7 for site "b," but is not part of the footprint for sites "c," "d," and "e." FHNA at T11 corresponds to position 5 for cleavage site "a," position 6 for "b," and position 7 for "c" (Figure 4D). FHNA at T11 ablates cleavage site "a," but not sites "b" and "c." This suggests that FHNA is tolerated at positions 6 and 7, but not at position 5 of the footprint. This is surprising because the DNA sugar at position 5 is in the RNA-like C3′-*endo* conformation that is mimicked by FHNA (Figure 4C). This suggests that the larger six-membered ring of FHNA is not accommodated within the hydrophobic DNA-binding channel or in the vicinity of the phosphate-binding pocket region of the catalytic domain of RNase H1.

Similarly, FHNA at A10 ablates "a" and "b"; C9 ablates "a," "b," and "c"; and T8 ablates "a," "b," "c," and "d" because it is located at positions 2, 3, 4, and 5 of the footprint for sites "a," "b," "c," and "d." Interestingly, FHNA at T8 does not ablate site "e" because it is now located at position 6 of the footprint for this cleavage site. Interestingly, cleavage site "e" is located at the 5′ edge of the gap region, where it is flanked with a cEt modification, which is "locked" in the RNA-like conformation. This tolerance for cEt at position 1 can be rationalized because the DNA sugar at position 1 in the crystal structure is in the RNA-like conformation that is mimicked by cEt.

This becomes apparent again when FHNA is incorporated at G7, which restores cleavage site "a." In this position, FHNA is at position 1 and cEt at position 7 of the footprint, where both modifications are tolerated. This ASO now effectively has a 5-base DNA gap that was previously shown to be the minimum length required for catalysis by RNase H1.[7] Along these lines, FHNA at T6 restores cleavage at sites "a" and "b"; FHNA at T5 restores "a," "b," and "c"; and FHNA at A4 restores "a," "b," "c," and "d," but ablates "e" because it is not tolerated at position 2 of the footprint.

The FHNA-modified ASOs versus the mismatched wtHTT RNA follow the same rules except that the T:G mismatch ablates cleavage sites "a" and "b" because RNase H1 does not tolerate mismatches in

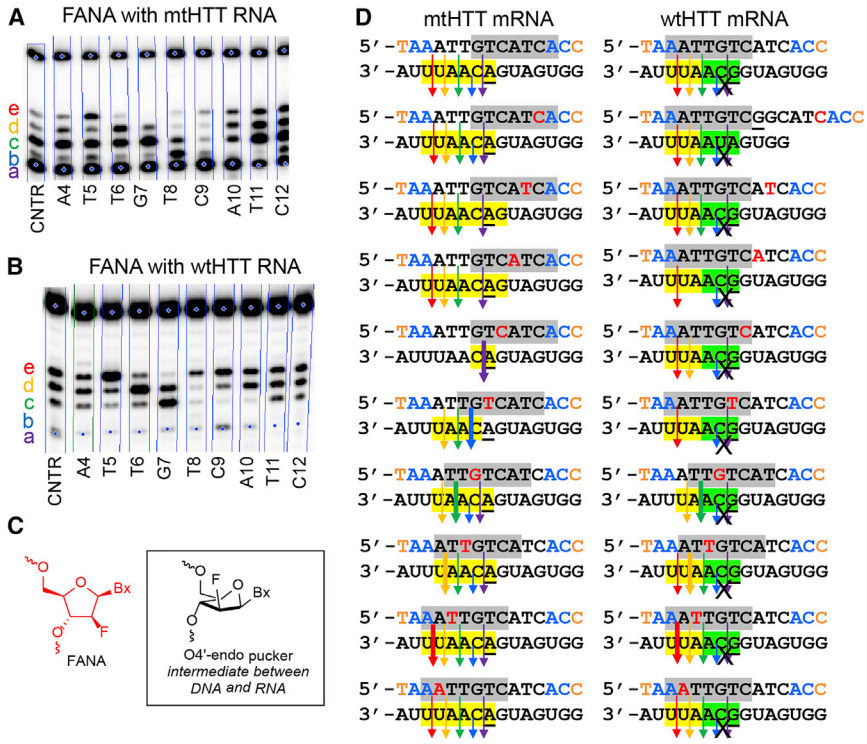


**Figure 5. RNase H Cleavage Patterns for FANA Gap-Modified ASOs**

(A and B) Analysis of human RNase H1 cleavage patterns for FANA gap-modified ASOs on (A) mtHTT RNA and (B) wtHTT RNA. (C) Structure and preferred conformation of the furanose ring in FANA. (D) Detailed analysis of the 7-nt footprint (gray shaded) on (D) ASO/mtHTT RNA and ASO/wtHTT RNA. The red letters depict position of FANA nucleotide, and the cleavage sites on the RNA are shown using arrows. The yellow shaded areas indicate sites where RNase H1 is able to cleave the RNA strand. The green shaded areas indicate sites where cleavage is ablated by the T:G mismatch corresponding to the SNP site.

the vicinity of the cleavage site. FHNA at positions T5, T6, and G7 ablate cleavage sites "c," "d," and "e," which translates to excellent allele selectivity in HD patient fibroblasts. However, FHNA at T6 and G7 also reduces overall cleavage of mtHTT RNA (Figure 2), which reduces potency, thus making the improved selectivity less interesting. Overall, all the observations for FHNA also apply for FRNA given that FHNA generally mimics FRNA in its conformational properties.[18] However, the furanose ring in FRNA is more flexible, resulting in less intense ablation of certain cleavage sites for both matched and mismatched duplexes (supporting Figure S5).

### Structural Analysis of the RNase H1 Cleavage Footprint for FANA Gap-Modified ASOs

Introducing FANA at C12, T11, and A10 had no noticeable effect on the RNase H cleavage patterns for mtHTT RNA relative to control ASO CNTR (Figures 5A and 5B). This suggests that FANA is tolerated at positions 4, 5, and 6 of the footprint. Slight ablation of "a" was seen with FANA at C12, suggesting that position 6 may not a preferred position for FANA. Interestingly, FANA at C9 almost completely focused RNase H1 cleavage at site "a," suggesting that position 3 in the footprint is a highly preferred site for FANA. This preference is also seen with FANA at T8, G7, T6, and T5, which corresponds to position 3 in the footprint for sites "b," "c," "d," and "e," respectively.

The strong preference for FANA at position 3 of the footprint is interesting because the DNA sugar at this position in the crystal structure is in the DNA-like C2′-*endo* conformation, which FANA can adopt but is not preferred.[20] This region of the crystal structure is where RNase H1 makes several intimate contacts with the nucleobases in the major groove, and the 2′-fluorine in the "ara" configuration in FANA might be able to modulate these interactions. Alternately, incorporation of a fluorine atom at the 2′ position of the furanose ring facilitates CH•••O type interactions between the 2′-hydrogen atom and the 4′-oxygen of the adjacent nucleotide.[35] This could potentially help pre-organize the DNA strand for more efficient cleavage.

The FANA-modified ASOs versus the mismatched wtHTT RNA follow the same rules except that the T:G mismatch ablates cleavage sites "a" and "b." However, because FANA is essentially tolerated at all positions of the footprint, complete ablation of RNase H1 cleavage on wtHTT RNA does not take place with FANA at any position in the gap. The improved selectivity seen with FANA at certain positions is more a result of enhanced potency versus the mutant allele as opposed to reduced activity versus the wild-type allele (Figure 2). However, the improved potency and selectivity with FANA (or FRNA) at A10 cannot be rationalized by analysis of cleavage patterns and suggests that additional factors may be involved in determining activity and selectivity for some ASOs.

### F-CeNA Substitution

F-CeNA-modified ASOs generally exhibit mtHTT reductions that are very similar to the control ASO at the positions tested (Figure 6). wtHTT reduction and allele selectivity are in most cases similar to FRNA and FHNA; however, because of the good mtHTT potency at position T6, F-CeNA exhibits the best properties of all the modifications examined when placed at this position. F-CeNA has an RNase H cleavage pattern that at most positions resembles FRNA; position T6, though, is a notable exception (Figure 6C) because mtHTT RNA cleavage bands at the main cleavage sites a and c are at similar intensities to CNTR ASO, whereas for FRNA they are significantly reduced. Thus, F-CeNA behaves similar to the

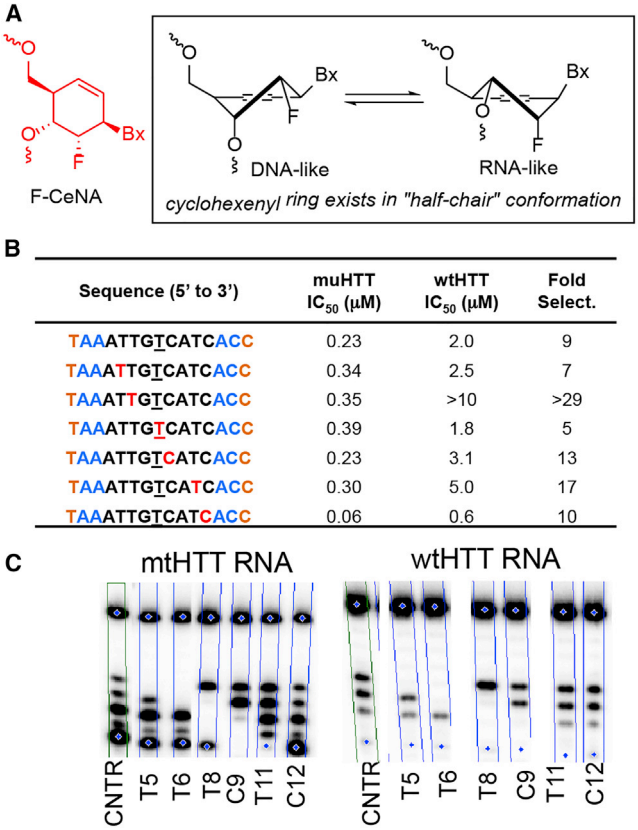


**Figure 6. Cell Culture Potency and RNase H Cleavage Patterns for F-CeNA Gap-Modified ASOs**

(A) Structure and preferred conformation of the furanose ring in F-CeNA. (B and C) Cell culture potency and allele selectivity (B), and human RNase H1 cleavage of mtHTT and wtHTT RNA hybridized to ASOs containing F-CeNA substitutions (C).

RNA-like modifications FRNA and FHNA, although it reduces RNase H-mediated RNA cleavage less than FRNA and FHNA.

### Comparing *North*-Methanocarba with F-*North*-Methanocarba

To further investigate the effect fluorine substitution can have on ASO properties, we investigated 2′-F-*North*-methanocarba (F-N-MC)[36] in the huntingtin SNP system. Because the non-fluorinated nucleotide *North*-methanocarba (N-MC) is conformationally restricted in the 3′-*endo* configuration,[37,38] fluorine substitution will have minimal influence on the sugar pucker (Figure 7A). Previous biophysical examination, however, showed that F-N-MC improved thermal stabilization with cRNA relative to parent nucleotide N-MC.[36] This stabilization was attributed to increased polarization of the nucleobase, likely resulting in improved Watson-Crick base-pairing and base stacking.[39]

F-N-MC-substituted ASOs are generally slightly more potent than parent N-MC ASOs in cell culture, whereas allele selectivity is similar (Figure 7C). Potency can be explained by the improved thermal stability of F-N-MC containing oligonucleotides relative to N-MC, but favorable interactions with RNase H cannot be ruled out. At one position, though, the trend is reversed. When modifying position T11, N-MC-substituted ASO is approximately 2-fold more potent than F-N-MC containing ASO (Figure 7C). This peculiar effect, though, can be explained by examining RNase H cleavage patterns (Figure 7B). Although the cleavage patterns are very similar for the two modifications, it is striking that at position T11, F-N-MC containing ASO has reduced cleavage at the normally main cleavage site "a." It is possible that the fluorine at position T11 has a negative impact on the RNase H footprint.

### Conclusions

This work has systematically investigated incorporation of fluorinated nucleotides in the gap region and finds a specific RNase H cleavage footprint for each nucleotide. Accordingly, it is possible to modulate RNase H cleavages when introducing fluorinated nucleotide modifications in the gap region using rational design principles to generate more mismatch-selective ASOs. Fluorination of nucleotides is a straightforward method to alter the properties of the nucleotides without adding much steric bulk. By incorporating such nucleotides systematically into the gap of an ASO targeting a *huntingtin* SNP, we have found multiple modifications and positions in the gap that significantly improve allele selectivity without affecting potency. Previous work has shown that at this SNP the ASO allele selectivity can simply be increased by decreasing the gap size from 9 to 7 nt.[17] Our work provides additional chemical design options to modulate the activity selectivity profile of SNP-targeting ASOs for the treatment of autosomal dominant disorders.

## MATERIALS AND METHODS

### ASO Solid-Phase Synthesis

Protected FRNA and FANA phosphoramidites were purchased from commercial sources. FHNA,[23] F-CeNA,[24] N-MC,[37] and F-N-MC[36] phosphoramidites were synthesized as described in the literature. ASOs were synthesized on an ABI 394 DNA/RNA Synthesizer on a 2 μmol scale using 5-methyl cytidine MOE-loaded primer support (215 μmol/g). Standard conditions were used for incorporation of DNA amidites, i.e., 3% dichloroacetic acid (DCA) in dichloromethylene (DCM) for deblocking; 1 M 4,5-dicyanoimidazole, 0.1 M *N*-methylimidazole in acetonitrile as activator, 0.1 M phosphoramidites dissolved in acetonitrile or, if necessary, in acetonitrile:toluene 1:1 (v:v), 2 × 4 min coupling times for coupling; Cap A: acetic anhydride in tetrahydrofuran (THF), Cap B: 10% 1-methylimidazole in THF/pyridine for capping and 0.2 M phenylacetyl disulfide in pyridine:acetonitrile 1:1 (v:v) aged for at least 48 hr. After synthesis, the final 4,4'-dimethoxytrityl (DMT) was cleaved, cyanoethyl-protecting groups were removed using triethylamine:acetonitrile 1:1 (v:v), and the remaining protecting groups were cleaved in concentrated aqueous ammonia at room temperature for 12 hr or until fully deprotected. ASOs were purified using ion exchange (IE)-HPLC using a linear gradient of buffer A (50 mM $NaHCO_3$ in acetonitrile:water 3:7 [v:v]) and buffer B (1.5 M NaBr, 50 mM $NaHCO_3$ in acetonitrile:water 3:7 [v:v]). Purified ASOs were

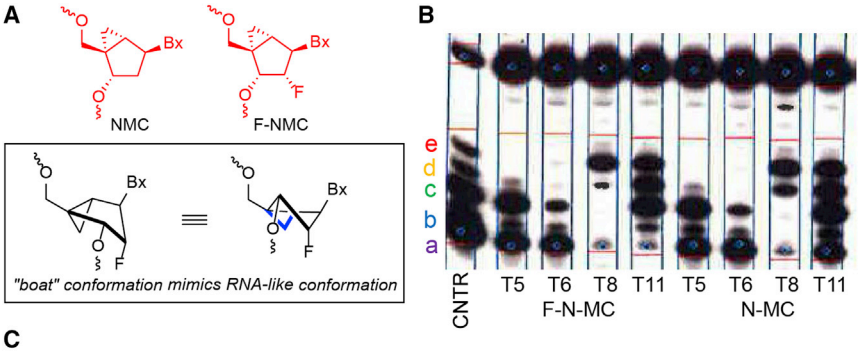


C

| Sequence (5' to 3') | NMC wt HTT $IC_{50}$ (μM) | NMC muHTT $IC_{50}$ (μM) | NMC Fold Select. | F-NMC wt HTT $IC_{50}$ (μM) | F-NMC muHTT $IC_{50}$ (μM) | F-NMC Fold Select. |
|---|---|---|---|---|---|---|
| TAAATTGTCATCACC | 0.23 | 2.0 | 9 | 0.23 | 2.0 | 9 |
| TAAATTGTCATCACC | 0.61 | >10 | >16 | 0.33 | >10 | >30 |
| TAAATTGTCATCACC | 3.9 | >10 | >3 | 2.0 | >10 | >5 |
| TAAATTGTCATCACC | 0.49 | 6.6 | 13 | 0.29 | 4.9 | 17 |
| TAAATTGTCATCACC | 0.38 | 8.2 | 22 | 0.84 | >10 | >12 |

**Figure 7. Comparing the Activity and Selectivity Profile of N-MC and F-N-MC Gap-Modified ASOs**
(A and B) Chemical structures and preferred conformation of the furanose ring of the two modifications (A); human RNase H1 cleavage of mtHTT RNA hybridized to ASOs containing N-MC or F-N-MC at either T in the gap (B). (C) Cell culture potency and allele selectivity.

desalted using C18 reverse-phase cartridges. ASO purity was determined by high performance liquid chromatography (HPLC) and identity by mass spectrometry (Table S1).

### Cell Culture mRNA Knockdown

GM04022 fibroblast cells were trypsinized and resuspended to a density of 400,000 cells/mL in growth medium prior to transfection with varying concentrations of ASO using electroporation (115 V, 6 ms). Cells were maintained at 37°C and 5% $CO_2$ in minimal essential medium containing 15% fetal bovine serum, non-essential amino acids, and penicillin-streptomycin. After 24 h the cells were washed with Dulbecco's PBS and lysed. RNA was extracted using the QIAGEN RNeasy96 kit, and human *HTT* mRNA alleles were quantitated using the qPCR assay C_2231945_10 at SNP rs362331 (Life Technologies). Mutant *huntingtin* (muHTT) and wtHTT mRNA levels were determined simultaneously using two different fluorophores: 6-carboxyfluorescein for muHTT and a fluorophore with structure not given by commercial vendor (VIC) for wtHTT mRNA. Quantitative rtPCRs were performed on an ABI 7900 HT instrument using the quantitect Prote rtPCR kit following the manufacturer's instructions. HTT mRNA levels were normalized relative to total RNA content measured using Ribogreen. All experiments were performed in duplicates, and data are expressed as means ± SD. Dose-response curves were analyzed using non-linear regression with normalized response and variable slope, and $IC_{50}$ values calculated using GraphPad Prism version 5. All dose-response curves are shown in the Supplemental Information (Figures S1–S4). Allele selectivity was calculated by dividing the $IC_{50}$ for inhibiting wtHTT with the $IC_{50}$ for inhibiting muHTT.

### Human RNase H1 Cleavage Pattern and Cleavage Intensity

RNA was 5′ end labeled with $^{32}P$ using 20 U of T4 polynucleotide kinase, 120 pmol (7000 Ci/mmol) of ($\gamma$-$^{32}P$)ATP, 40 pmol of RNA, 70 mM Tris-HCl, 10 mM $MgCl_2$, and 50 mM dithiothreitol at pH 7.6. The labeling reaction was incubated at 37°C for 30 min followed by heating at 90°C for 1 min. Labeled RNA was purified using 12% denaturing polyacrylamide gel. ASO (200 nM), unlabeled 19-mer RNA (100 nM), and a small amount of $^{32}P$-labeled RNA was mixed in hybridization buffer (20 mM Tris-HCl, 20 mM KCl [pH 7.5]) and heated to 90°C for 2 min. To the hybridization mixture was added 0.1 mM (*tris*(2-carboxyethyl)phosphine) (TCEP), 1 mM $MgCl_2$, and 40 U of RNaseOUT, and it was incubated at 37°C for 1 hr. The human RNase H1 enzyme was incubated in dilution buffer (20 mM Tris-HCl, 50 mM KCl, 2 mM TCEP [pH 7.5]) for 1 hr at room temperature. Enzyme solution (4% volume relative to duplex solution) was added to duplex solution and incubated at 37°C. After 6 min, reaction was quenched by addition of loading buffer and snap-frozen on dry ice. Cleavage products were separated using 12% denaturing polyacrylamide gel electrophoresis, and products were quantitated on a Phosphor-Imager. RNA sequences used herein were: 19-mer muHTT RNA, 5′-CUGGUGAUGACAAUUUAUU-3′; 19-mer wtHTT RNA, 5′-CUGGUGAUGGCAAUUUAUU-3′. Identity of RNA cleavage products was determined by separating cleavage products on ion-pairing reverse-phase HPLC and determining cleavage products using electrospray ionization mass spectrometry as previously described.[17]

## SUPPLEMENTAL INFORMATION

Supplemental Information includes five figures and one table and can be found with this article online at http://dx.doi.org/10.1016/j.omtn.2017.02.001.

## AUTHOR CONTRIBUTIONS

Synthesis of modified nucleotides, T.A.D., M.E.J.; ASO Synthesis and Cell Culture Studies, M.E.O.; RNase H1 Experiments, J.N., W.L.; Manuscript Preparation, M.E.O., P.P.S.; Manuscript Proof Reading and Suggestions, M.E.O., J.N., T.A.D., W.L., M.E.J., E.E.S., P.P.S.

## ACKNOWLEDGMENTS

We acknowledge Prof. Marcin Nowotny for critical reading of the manuscript and Dr. Stanley Crooke for many useful discussions.

## REFERENCES


1. Bennett, C.F., and Swayze, E.E. (2010). RNA targeting therapeutics: molecular mechanisms of antisense oligonucleotides as a therapeutic platform. Annu. Rev. Pharmacol. Toxicol. *50*, 259–293.
2. Zamecnik, P.C., and Stephenson, M.L. (1978). Inhibition of Rous sarcoma virus replication and cell transformation by a specific oligodeoxynucleotide. Proc. Natl. Acad. Sci. USA *75*, 280–284.
3. Crooke, S.T., ed. (2008). Antisense Drug Technology: Principles, Strategies, and Applications, Second Edition (CRC Press LLC).
4. Kurreck, J. (2003). Antisense technologies. Improvement through novel chemical modifications. Eur. J. Biochem. *270*, 1628–1644.
5. Crooke, S.T., and Geary, R.S. (2013). Clinical pharmacological properties of mipomersen (Kynamro), a second generation antisense inhibitor of apolipoprotein B. Br. J. Clin. Pharmacol. *76*, 269–276.
6. Shibahara, S., Mukai, S., Nishihara, T., Inoue, H., Ohtsuka, E., and Morisawa, H. (1987). Site-directed cleavage of RNA. Nucleic Acids Res. *15*, 4403–4415.
7. Monia, B.P., Lesnik, E.A., Gonzalez, C., Lima, W.F., McGee, D., Guinosso, C.J., Kawasaki, A.M., Cook, P.D., and Freier, S.M. (1993). Evaluation of 2′-modified oligonucleotides containing 2′-deoxy gaps as antisense inhibitors of gene expression. J. Biol. Chem. *268*, 14514–14522.
8. Wan, W.B., and Seth, P.P. (2016). The medicinal chemistry of therapeutic oligonucleotides. J. Med. Chem. *59*, 9645–9667.
9. Wahlestedt, C., Salmi, P., Good, L., Kela, J., Johnsson, T., Hökfelt, T., Broberger, C., Porreca, F., Lai, J., Ren, K., et al. (2000). Potent and nontoxic antisense oligonucleotides containing locked nucleic acids. Proc. Natl. Acad. Sci. USA *97*, 5633–5638.
10. Seth, P.P., Siwkowski, A., Allerson, C.R., Vasquez, G., Lee, S., Prakash, T.P., Wancewicz, E.V., Witchell, D., and Swayze, E.E. (2009). Short antisense oligonucleotides with novel 2′-4′ conformationaly restricted nucleoside analogues show improved potency without increased toxicity in animals. J. Med. Chem. *52*, 10–13.
11. Lima, W.F., Nichols, J.G., Wu, H., Prakash, T.P., Migawa, M.T., Wyrzykiewicz, T.K., Bhat, B., and Crooke, S.T. (2004). Structural requirements at the catalytic site of the heteroduplex substrate for human RNase H1 catalysis. J. Biol. Chem. *279*, 36317–36326.
12. Lima, W.F., Rose, J.B., Nichols, J.G., Wu, H., Migawa, M.T., Wyrzykiewicz, T.K., Vasquez, G., Swayze, E.E., and Crooke, S.T. (2007). The positional influence of the helical geometry of the heteroduplex substrate on human RNase H1 catalysis. Mol. Pharmacol. *71*, 73–82.
13. Østergaard, M.E., Kumar, P., Nichols, J., Watt, A., Sharma, P.K., Nielsen, P., and Seth, P.P. (2015). Allele-selective inhibition of mutant Huntingtin with 2-Thio- and C5-triazolylphenyl-deoxythymidine-modified antisense oligonucleotides. Nucleic Acid Ther. *25*, 266–274.
14. Østergaard, M.E., Gerland, B., Escudier, J.M., Swayze, E.E., and Seth, P.P. (2014). Differential effects on allele selective silencing of mutant huntingtin by two stereoisomers of α,β-constrained nucleic acid. ACS Chem. Biol. *9*, 1975–1979.
15. Southwell, A.L., Skotte, N.H., Kordasiewicz, H.B., Østergaard, M.E., Watt, A.T., Carroll, J.B., Doty, C.N., Villanueva, E.B., Petoukhov, E., Vaid, K., et al. (2014). In vivo evaluation of candidate allele-specific mutant huntingtin gene silencing antisense oligonucleotides. Mol. Ther. *22*, 2093–2106.
16. Gagnon, K.T., Pendergraff, H.M., Deleavey, G.F., Swayze, E.E., Potier, P., Randolph, J., Roesch, E.B., Chattopadhyaya, J., Damha, M.J., Bennett, C.F., et al. (2010). Allele-selective inhibition of mutant huntingtin expression with antisense oligonucleotides targeting the expanded CAG repeat. Biochemistry *49*, 10166–10178.
17. Østergaard, M.E., Southwell, A.L., Kordasiewicz, H., Watt, A.T., Skotte, N.H., Doty, C.N., Vaid, K., Villanueva, E.B., Swayze, E.E., Bennett, C.F., et al. (2013). Rational design of antisense oligonucleotides targeting single nucleotide polymorphisms for potent and allele selective suppression of mutant Huntingtin in the CNS. Nucleic Acids Res. *41*, 9634–9650.
18. Østergaard, M.E., Dwight, T., Berdeja, A., Swayze, E.E., Jung, M.E., and Seth, P.P. (2014). Comparison of duplex stabilizing properties of 2′-fluorinated nucleic acid analogues with furanose and non-furanose sugar rings. J. Org. Chem. *79*, 8877–8881.
19. Manoharan, M., Akinc, A., Pandey, R.K., Qin, J., Hadwiger, P., John, M., Mills, K., Charisse, K., Maier, M.A., Nechev, L., et al. (2011). Unique gene-silencing and structural properties of 2′-fluoro-modified siRNAs. Angew. Chem. Int. Ed. Engl. *50*, 2284–2288.
20. Wilds, C.J., and Damha, M.J. (2000). 2′-Deoxy-2′-fluoro-beta-D-arabinonucleosides and oligonucleotides (2′F-ANA): synthesis and physicochemical studies. Nucleic Acids Res. *28*, 3625–3635.
21. Damha, M.J., Wilds, C.J., Noronha, A., Brukner, I., Borkow, G., Arion, D., and Parniak, M.A. (1998). Hybrids of RNA and arabinonucleic acids (ANA and 2′F-ANA) are substrates of ribonuclease H. J. Am. Chem. Soc. *120*, 12976–12977.
22. Min, K.L., Viazovkina, E., Galarneau, A., Parniak, M.A., and Damha, M.J. (2002). Oligonucleotides comprised of alternating 2′-deoxy-2′-fluoro-beta-D-arabinonucleosides and D-2′-deoxyribonucleosides (2′F-ANA/DNA 'altimers') induce efficient RNA cleavage mediated by RNase H. Bioorg. Med. Chem. Lett. *12*, 2651–2654.
23. Egli, M., Pallan, P.S., Allerson, C.R., Prakash, T.P., Berdeja, A., Yu, J., Lee, S., Watt, A., Gaus, H., Bhat, B., et al. (2011). Synthesis, improved antisense activity and structural rationale for the divergent RNA affinities of 3′-fluoro hexitol nucleic acid (FHNA and Ara-FHNA) modified oligonucleotides. J. Am. Chem. Soc. *133*, 16642–16649.
24. Seth, P.P., Yu, J., Jazayeri, A., Pallan, P.S., Allerson, C.R., Østergaard, M.E., Liu, F., Herdewijn, P., Egli, M., and Swayze, E.E. (2012). Synthesis and antisense properties of fluoro cyclohexenyl nucleic acid (F-CeNA), a nuclease stable mimic of 2′-fluoro RNA. J. Org. Chem. *77*, 5074–5085.
25. Pallan, P.S., Marquez, V.E., and Egli, M. (2012). The conformationally constrained N-methanocarba-dT analogue adopts an unexpected C4′-exo sugar pucker in the structure of a DNA hairpin. Biochemistry *51*, 2639–2641.
26. Carroll, J.B., Warby, S.C., Southwell, A.L., Doty, C.N., Greenlee, S., Skotte, N., Hung, G., Bennett, C.F., Freier, S.M., and Hayden, M.R. (2011). Potent and selective antisense oligonucleotides targeting single-nucleotide polymorphisms in the Huntington disease gene / allele-specific silencing of mutant huntingtin. Mol. Ther. *19*, 2178–2185.
27. Nowotny, M., Gaidamakov, S.A., Ghirlando, R., Cerritelli, S.M., Crouch, R.J., and Yang, W. (2007). Structure of human RNase H1 complexed with an RNA/DNA hybrid: insight into HIV reverse transcription. Mol. Cell *28*, 264–276.
28. Li, F., Sarkhel, S., Wilds, C.J., Wawrzak, Z., Prakash, T.P., Manoharan, M., and Egli, M. (2006). 2′-Fluoroarabino- and arabinonucleic acid show different conformations, resulting in deviating RNA affinities and processing of their heteroduplexes with RNA by RNase H. Biochemistry *45*, 4141–4152.
29. Orban, T.I., and Izaurralde, E. (2005). Decay of mRNAs targeted by RISC requires XRN1, the Ski complex, and the exosome. RNA *11*, 459–469.
30. Lima, W.F., De Hoyos, C.L., Liang, X.H., and Crooke, S.T. (2016). RNA cleavage products generated by antisense oligonucleotides and siRNAs are processed by the RNA surveillance machinery. Nucleic Acids Res. *44*, 3351–3363.
31. Wu, H., Sun, H., Liang, X., Lima, W.F., and Crooke, S.T. (2013). Human RNase H1 is associated with protein P32 and is involved in mitochondrial pre-rRNA processing. PLoS ONE *8*, e71006.
32. Liang, X.H., Sun, H., Shen, W., and Crooke, S.T. (2015). Identification and characterization of intracellular proteins that bind oligonucleotides with phosphorothioate linkages. Nucleic Acids Res. *43*, 2927–2945.
33. Shen, W., Liang, X.H., Sun, H., and Crooke, S.T. (2015). 2′-Fluoro-modified phosphorothioate oligonucleotide can cause rapid degradation of P54nrb and PSF. Nucleic Acids Res. *43*, 4569–4578.
34. Miller, C.M., Donner, A.J., Blank, E.E., Egger, A.W., Kellar, B.M., Østergaard, M.E., Seth, P.P., and Harris, E.N. (2016). Stabilin-1 and Stabilin-2 are specific receptors for the cellular internalization of phosphorothioate-modified antisense oligonucleotides (ASOs) in the liver. Nucleic Acids Res. *44*, 2782–2794.
35. Martin-Pintado, N., Deleavey, G.F., Portella, G., Campos-Olivas, R., Orozco, M., Damha, M.J., Gonzalez, C., and Backbone, F.C.-H. (2013). O hydrogen bonds in 2′F-substituted nucleic acids. Angew. Chem. Int. Ed. *52*, 12065–12068.
36. Jung, M.E., Dwight, T.A., Vigant, F., Østergaard, M.E., Swayze, E.E., and Seth, P.P. (2014). Synthesis and duplex-stabilizing properties of fluorinated N-methanocarbathymidine analogues locked in the C3′-endo conformation. Angew. Chem. Int. Ed. Engl. *53*, 9893–9897.

37. Marquez, V.E., Siddiqui, M.A., Ezzitouni, A., Russ, P., Wang, J., Wagner, R.W., and Matteucci, M.D. (1996). Nucleosides with a twist. Can fixed forms of sugar ring pucker influence biological activity in nucleosides and oligonucleotides? J. Med. Chem. *39*, 3739–3747.

38. Maier, M.A., Choi, Y., Gaus, H., Barchi, J.J., Jr., Marquez, V.E., and Manoharan, M. (2004). Synthesis and characterization of oligonucleotides containing conformationally constrained bicyclo[3.1.0]hexane pseudosugar analogs. Nucleic Acids Res. *32*, 3642–3650.

39. Patra, A., Paolillo, M., Charisse, K., Manoharan, M., Rozners, E., and Egli, M. (2012). 2′-Fluoro RNA shows increased Watson-Crick H-bonding strength and stacking relative to RNA: evidence from NMR and thermodynamic data. Angew. Chem. Int. Ed. Engl. *51*, 11863–11866.